Development and Validation of Inverse Flight Dynamics Simulation for Helicopter Maneuver

Raghavendra Prasad
Graduate Student
raghavv@iitk.ac.in

Abhishek
Assistant Professor
abhish@iitk.ac.in

Department of Aerospace Engineering
Indian Institute of Technology Kanpur
Kanpur, India

ABSTRACT

This paper discusses the development, implementation and validation of a robust inverse flight dynamics simulation for helicopters undergoing steady and unsteady maneuvers. An algorithm based on integration based inverse simulation approach is implemented which regulates the required vehicle accelerations necessary to track the desired trajectory by adjusting the controls required by the helicopter. Helicopter dynamics model consists of individual rigid blades with flapping dynamics and quasi-steady aerodynamics. The analysis has the option of using airfoil C_l and C_d lookup tables for non-linear aerodynamic modelling, if such tables are available. The present inverse flight dynamics analysis is verified and validated using available flight test and simulated results for literature for UH-60A Black Hawk and Westland Lynx helicopters respectively. The derived procedure is used to satisfactorily predict the pilot input controls and shaft orientation angles that are required to fly several maneuvers including pull-up, hurdle-hop, pop-up, bob-up and pirouette.

NOTATIONS

u : Control vector
u,v,w : Tanslational velocity in body frame
p,q,r : Angular velocity in body frame
x : System state vector
y : Output vector
V_f : Resultant velocity (m/s)
V_{max} : Maximum velocity (m/s)
V_{tip} : Blade tip velocity (m/s)
V : Velocity (m/s)
t : Time (s)
t_m : Maneuver time (s)
h : Altitude (m)
m : Helicopter mass (kg)
X_e, Y_e, Z_e : Helicopter position in gravity axes
θ_0 : Blade collective pitch
θ_{1c} : Blade lateral cyclic pitch
θ_{1s} : Blade longitudinal cyclic pitch
α_s : Longitudinal shaft tilt
ϕ_s : Lateral shaft tilt
$\dot{a}$: Time rate of change of any variable a
ω: Angular velocity of main rotor (rad/s)
Ω: Angular velocity of helicopter (rad/s)

Presented at the 4th Asian/Australian Rotorcraft Forum, IISc, India, November 16–18, 2015.

INTRODUCTION

Study of helicopters, for either the handling qualities or the prediction of helicopter blade loads, requires the knowledge of control inputs necessary to fly / simulate the desired flight. Trim analysis can be performed to predict the input controls for steady flight in which controls are obtained by targeting steady equilibrium of the vehicle. But in case of unsteady maneuvers, where states are instantaneous and transient, trim analysis cannot be performed because states are also to be determined simultaneously with controls. Derivation of time history of pilot input controls required for flying or simulating an unsteady maneuvers is called inverse simulation. This is opposite to usual forward simulation where the input controls are known and the output response to prescribed input is of interest. During inverse simulation, the desired output response, such as, trajectory, is known and the input controls required to achieve the desired output response is calculated.

Several successful attempts have been made to use inverse flight dynamic simulation for helicopter application following the demonstration of its usefulness in deriving controls for fixed wing aircraft (Refs. 1,2). Several methods have been studied by researchers over the years for inverse flight dynamics modelling. All these approaches available in literature can be broadly classified into three categories: 1) differentiation approach, 2) integration approach and 3) global optimization based methods.

Thomson and Bradley (Refs. 3,4) were among the first re-

searchers to develop an inverse flight dynamics simulation algorithm "HELINV" for rotorcraft application. Their approach was based on numerical differentiation of states at every time step to evaluate the time derivatives of the states. This allowed them to transform the governing differential equations to algebraic equations which could be solved to obtain the control angles. Despite being model dependent and sensitive to time step size this method highlighted the usefulness of inverse simulation as an effective tool in helicopter flight dynamics by analyzing several unsteady maneuvers.

Hess et al. (Refs. 5, 6) formulated integration inverse method in which states are modified using repeated numerical integration of the equations of motion during a constrained time step by keeping the controls constant. At the end of the time step the controls are modified using Newton Raphson to reduce the error between the desired and achieved states. While, it is an order of magnitude slower than the differentiation based approach, it is independent of rotor dynamics model and allows for its refinement without any need for altering the solution procedure. Lin (Ref. 7) reported the numerical issues such as constrained oscillations associated with this approach. De Matteis et al. (Ref. 8) replaced the Newton-Raphson step with local optimization procedure, eliminating constrained oscillations mentioned earlier in this process. In this approach, controls are calculated by minimizing a cost function which is defined based on required performance indices. This is done using either classical finite difference Newton method or Sequential Quadratic Programming (SQP) algorithm. A "two-timescale" method of integration based inverse simulation was proposed by Avanzini and de Matteis (Ref. 9) that reduces the computational effort by decoupling and solving the rotational and translational dynamics separately. But this method adds certain level of inaccuracies to the solution.

Global optimization method, proposed by Celi (Ref. 10), operates on a whole family of possible trajectories (and therefore, of pilot command time histories) unlike the methods derived earlier. Based of required performance criteria the best trajectory and corresponding set of controls are chosen to carry out a specific maneuver. However, this requires significant amount of function evaluations, resulting in significant computational penalty. A general optimization method studied by Lee and Kim (Ref. 11) used time-domain finite element method to discretize the governing equations for blade response and numerical solution for control angles is obtained through least square optimization. Lu and Murray-Smith (Ref. 12) developed an inverse simulation method based on sensitivity-analysis theory in which a Jacobian matrix is calculated by solving sensitivity equation. This methodology overcomes numerical as well as inputoutput redundancy problem that arise in traditional methodologies.

In addition to gradient based method, global optimization may be achieved by using genetic algorithm based approach. This obviates the need for calculation of gradients but the convergence is typically slower. A genetic algorithm based approach was used for inverse simulation of pirouette and slalom manoeuvres by Guglieri and Mariano (Ref. 13) to successfully demonstrate the precise tracking of the prescribed trajectories with reasonable control inputs. A Hybrid Genetic Algorithm is also used for helicopter trim research, which tries to combine the reliability of the Genetic Algorithm with the speed of the quasi-Newton iterative approach. The calculation in started with Genetic Algorithm and switches to quasi-Newton method when a desired fitness level is achieved (Ref. (Ref. 14)). This allows the algorithm to converge in a larger range with a faster convergence velocity.

In this paper, focus is on preliminary development of robust inverse flight dynamics simulation for estimating control angles for wide range of maneuvers performed by helicopters. The integration based approach is used for the present analysis due to its ease of implementation and independence from helicopter rotor dynamics models. The long term goal is to progressively refine the rotor dynamics and aerodynamics models within the analysis and understand their effect on the prediction capability of the model. The current analysis is first validated by simulation of aggressive pull-up maneuver for UH-60A Black Hawk helicopter, for which flight test data is available in public domain. The control prediction capability of the present analysis is then verified for other maneuvers such as pop-up and hurdle-hop maneuvers for Westland Lynx helicopter with available simulated results from literature. Finally, bob-up and pirouette maneuvers are also simulated.

APPROACH

Integration based inverse flight dynamics simulation approach is chosen for present analysis. In this approach vehicle states, in body reference frame, are systematically integrated over a constrained time step, transformed into earth fixed reference frame and controls are modified by reducing the error between simulated and required velocity at the end of time step using Newton-Raphson. The main advantage of this procedure is model can be separated from simulation algorithm that makes the procedure very flexible in studying the effect of various modelling refinements. This procedure is explained below.

A dynamic system can be described as a function of states and controls

$$\dot{\mathbf{x}} = f(\mathbf{x}, \mathbf{u}) \tag{1}$$

by using the updated states from the above equation, instantaneous system output can be derived from the following equation, provided that time history of system controls is given.

$$\mathbf{y} = g(\mathbf{x}) \tag{2}$$

But in a situation where time history of desired output is known and sequence of controls that drive the system to achieve the given output are to be determined, system dynamics must be inverted. The basis for inverse simulation can be obtained by differentiating the output equation with respect to time until the required controls appear in the resulting equation.

$$\dot{\mathbf{y}} = \frac{dg}{d\mathbf{x}}\dot{\mathbf{x}} \tag{3}$$

$$\dot{\mathbf{y}} = \frac{dg}{d\mathbf{x}} f(\mathbf{x}, \mathbf{u}) \tag{4}$$

controls can be calculated by inverting the above equation, which takes the form

$$\mathbf{u} = h(\mathbf{x}, \dot{\mathbf{y}}) \tag{5}$$

thus controls can be written as function of system output and corresponding states.

For the present analysis, system is represented by Newton-Euler equations, shown below, governing the rigid body dynamics of helicopter. Though these equations are general for any rigid body, the derivation of external forces X, Y, Z and moments L, M, N, acting along the three body fixed axes of the helicopter, are carried out using a helicopter rotor dynamics model.

Force equilibrium equations

$$m(\dot{u} + qw - rv) + mg\sin\theta = X \tag{6}$$
$$m(\dot{v} + ru - pw) - mg\sin\phi\cos\theta = Y \tag{7}$$
$$m(\dot{w} + pv - qu) - mg\cos\phi\cos\theta = Z \tag{8}$$

Moment equilibrium equations

$$I_{xx}\dot{p} - (I_{yy} - I_{zz})qr + I_{yz}(r^2 - q^2) - I_{xz}(pq + \dot{r}) + I_{xy}(pr - \dot{q}) = L \tag{9}$$

$$I_{yy}\dot{q} - (I_{zz} - I_{xx})pr + I_{xz}(p^2 - r^2) - I_{xy}(qr + \dot{p}) + I_{yz}(pq - \dot{r}) = M \tag{10}$$

$$I_{zz}\dot{r} - (I_{xx} - I_{yy})pq + I_{xy}(q^2 - p^2) - I_{yz}(pr + \dot{q}) + I_{xz}(qr - \dot{p}) = N \tag{11}$$

Kinematics equations

$$p = \dot{\phi} - \dot{\psi}\sin\theta \tag{12}$$
$$q = \dot{\theta}\cos\phi + \dot{\psi}\sin\phi cos\theta \tag{13}$$

Full six degrees of freedom of the vehicle are considered for current analysis: all three translational and rotational degrees of freedom. But it should be noted that the yaw degree of freedom does not play a significant role for the maneuvers being analyzed in this research which primarily involve motion in vertical-longitudinal plane and any out of plane motion is of small magnitude.

In case of a conventional helicopter, the key system states of interest are

$$\mathbf{x} = \{u, v, w, p, q, r\} \tag{14}$$

and the control inputs that need to be determined are

$$\mathbf{u} = \{\theta_0, \theta_{1c}, \theta_{1s}, \theta_{tr}\}^T \tag{15}$$

and the desired output $\mathbf{y}$ would be the maneuver trajectory that is to be performed by aircraft. The definition and modeling of various maneuvers is discussed later in text.

Integration Inverse Method

The simulation is initiated by dividing the entire trajectory for the maneuver into small steps. Then at each instance of time, an estimate of the change in the amplitude of control displacement required to move the aircraft to the next point is carried out. It is assumed that the controls are constant for each time interval [$\mathbf{t}_k$,$\mathbf{t}_{k+1}$]. Initial guesses of the controls $\mathbf{u}(\mathbf{t}_k)$ are used for the forward simulation. The output $\mathbf{y}(\mathbf{t}_{k+1})$ obtained from the simulation is compared with the desired output $\mathbf{y}^*(\mathbf{t}_{k+1})$. Based on the errors, the guessed controls are modified using, for example, Newton's method. The process repeats itself until the simulation result converges to the desired trajectory at $\mathbf{t}_{k+1}$. Then the analysis is moved to the next time step.

A step by step procedure describing the integration inverse approach is included below:

1. The set of equations of motion is derived.
2. The initial value of the State Vector is calculated.
3. The Desired Trajectory is defined.
4. The trajectory is descretized into Constrained Time Steps.
5. Each constrained time step is further descretized into Elemental Time Steps.
6. The initial guess of the control vector is made by solving the trim problem for initial steady state.
7. The State vector is updated by forward simulation to obtain the actual output at the Constrained Time Step, considering the control vector as constant throughout the entire Constrained Time Step.
8. The deviation of the actual trajectory from the desired trajectory (at Constrained Time Step) is calculated and the Control Vector is updated.
9. The above mentioned steps are repeated until the deviation of the actual trajectory from the desired trajectory reaches a predetermined minute value, which results in the Required Control Vector that is to be applied initially (i.e., at the previous Constrained Step) to achieve approximately desired trajectory at the Constrained Step-1 (i.e., at the new Constrained Step).
10. The above iterative procedure is continued for the remaining constrained steps. A flowchart describing the implementation of integration inverse simulation procedure to unsteady maneuver is shown in Fig. 1.

Where the notations have their usual meaning, e.g. ϕ, θ, and ψ respectively denote the roll, pitch, and yaw attitudes of the helicopter.

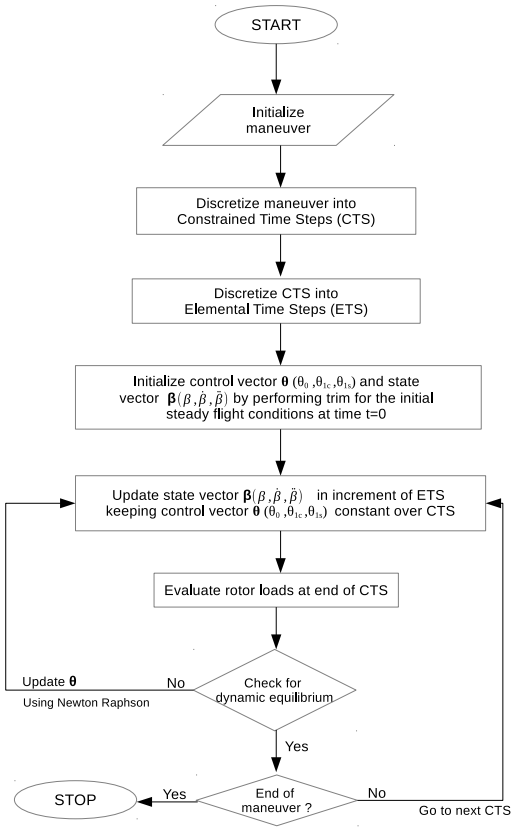

Fig. 1. Flow chart depicting integration inverse simulation procedure

Helicopter Dynamics Model

The main rotors of the two helicopters, UH-60A Black Hawk and Westland Lynx, being simulated are modeled as fully articulated rotors with rigid blades with hinge offset and having only the flap degree of freedom. Appropriate root spring is selected to match the first flap frequency. The individual blades are modeled with linear twist and root cut-out. The rotor longitudinal pre-shaft tilt angle is also considered. Though a standard symmetric airfoil with lift curve slope of 5.73 is used over the entire rotor blade for Westland Lynx helicopter, two different airfoil tables corresponding to SC1095 and SC1094R8, are used for UH-60A Black Hawk rotor.

Tail rotor model is a simple model based on Blade Element Theory (BET) while the tail rotor inflow is calculated using uniform inflow. The side force contribution of the tail rotor is included in the equation of motion to compensate for the main rotor torque required to maintain stable yaw.

Since, the lookup tables for the airfoils used on the UH-60A Black Hawk Helicopter is available in public domain, it is used for non-linear quasi-steady aerodynamic calculations during this analysis. The detailed rotor geometry and blade properties data for UH-60A is taken from (Refs. 15–18).

The flight test helicopter had test instrumentation and other fittings, the parasite drag of the helicopter is therefore represented using a quadratic function available in (Ref. 19): $D/q(ft^2) = 35.14 + 0.016(1.66\alpha_s)^2$ where, q is the dynamic pressure and α_s represents the helicopter pitch attitude.

Only linear aerodynamics is considered for Westland Lynx due to unavailability of the actual airfoil table. Drees model is used for inflow calculation and blade flap dynamics equations are solved using Newmark's algorithm.

The relevant parameters used for helicopter dynamics modeling are shown in Table 1.

Table 1. Helicopter parameters used for inverse simulation

Main Rotor	UH-60A	Westland Lynx
Number of Blades, N	4	4
Radius, R (m)	8.17	6.4
Blade Chord, c (m)	0.52	0.391
Rotational Speed, Ω (rad/s)	27.01	35.63
Longitudinal Shaft Tilt (degs.)	-3	0
Linear Blade Twist, θ_{tw} (rad/m)	-0.3142	-0.14
Lock Number, γ	6.33	7.12
Blade Flap Frequency, ν_β	1.04	1.07
Fuselage		
Gross Weight (kg)	7876.18	4313.7
Roll Inertia, I_{xx} (kg-m^2)	4659	2767.1
Pitch Inertia, I_{yy} (kg-m^2)	38512	13904.5
Yaw Inertia, I_{zz} (kg-m^2)	36800	12208.8
Product of Inertia, I_{xz} (kg-m^2)	1882	2034.8
Tail Rotor		
Number of Blades, N_t	4	4
Radius, R_t (m)	1.6764	1.106
Blade Chord, c_t (m)	0.24	0.180
Rotational Speed, Ω_t (rad/s)	124.62	193.103
Linear Blade Twist, θ_{tw} (rad/m)	0	0

Maneuver Model

Since the purpose of inverse simulation is to derive the time history of controls required by the system model to respond as per the pre-defined output, the definition of desired output is a very important step. As explained in (Ref. 20), the maneuver trajectories can be typically modeled as smooth polynomial functions of time in terms of velocity of vehicle defined in earth fixed frame of reference. In the present analysis five maneuvers namely pull-up, pop-up, hurdle-hop, bob-up and pirouette maneuvers are simulated.

Pop-up Maneuver

As shown in Fig. 2, the pop-up maneuver involves clearing an obstacle by a rapid controlled change of altitude over some horizontal distance. The trajectory can be defined by a polynomial equation with some boundary conditions. A fifth-order polynomial has been found to satisfy these boundary

conditions (Ref. 20) and is shown below.

$$Z_e(t) = -h\left[6\left(\frac{t}{t_m}\right)^5 - 15\left(\frac{t}{t_m}\right)^4 + 10\left(\frac{t}{t_m}\right)^3\right] \quad (16)$$

$$\dot{X}_e(t) = \sqrt{V_f^2 - \dot{Z}_e(t)^2} \quad (17)$$

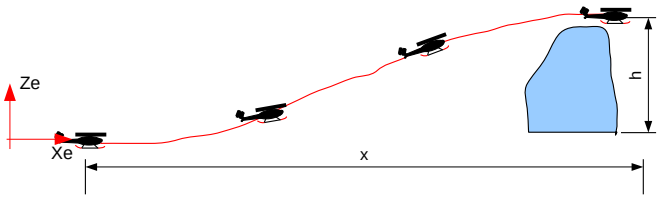

Fig. 2. Picture depicting pop-up maneuver

A pop maneuver of 8 second duration is chosen for the present simulation, which is initiated from a steady velocity of 41.15 m/s to reach an altitude of 25 m. It is a constant forward velocity maneuver in which the resultant velocity of logitudinal and vertical motions remain constant throughout the maneuver. The helicopter is accelerated over first half duration of maneuver which is then followed by a deceleration in vertical direction resulting in a gain of desired altitude.The helicopter would come back to its initial steady velocity state by the end of maneuver. The variation of longitudinal and vertical non-dimensional acceleration of helicopter is shown as a function of time in Fig. 3

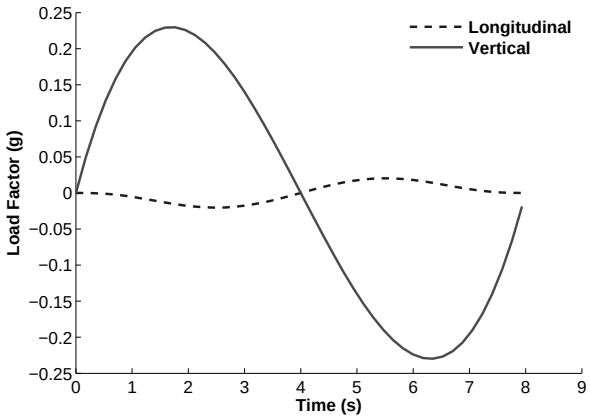

Fig. 3. Load factor variation for Pop-up maneuver

Hurdle-hop Maneuver

The hurdle-hop maneuver, as shown in Fig. 4, involves clearing an obstacle of height h and returning back to the original altitude over some specified distance, x. A polynomial equation describing the hurdle-hop maneuver is given as (Ref. 20):

$$Z_e(t) = -64h\left[\left(\frac{t}{t_m}\right)^3 - 3\left(\frac{t}{t_m}\right)^2 + 3\left(\frac{t}{t_m}\right) - 1\right]\left(\frac{t}{t_m}\right)^3 \quad (18)$$

$$\dot{X}_e(t) = \sqrt{V_f^2 - \dot{Z}_e(t)^2} \quad (19)$$

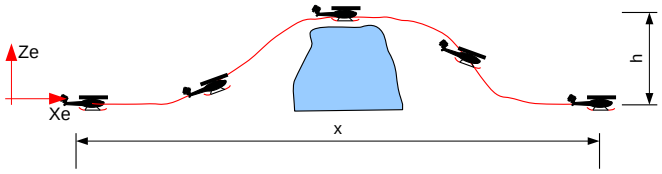

Fig. 4. Picture depicting hurdle-hop maneuver

For the present simulation this maneuver starts with a steady velocity of 41.15 m/s and reaches an altitude of 50 m during the first half of the maneuver. Like pop-up maneuver this is also a constant forward velocity maneuver in which climbing velocity becomes zero at the highest altitude point, from where helicopter starts descending and gradually reaches back to its initial altitude. This maneuver is carried out over a period of 17.5 seconds. The variation of longitudinal and vertical non-dimensional acceleration of helicopter is shown as a function of time in Fig. 5

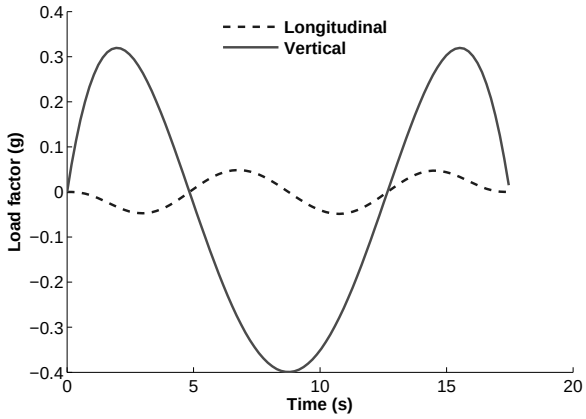

Fig. 5. Load factor variation for hurdle-hop maneuver

Pull-up Maneuver

Pull-up maneuver simulated here is for UH-60A Black Hawk helicopter. This is a terrain avoidance maneuver and is initiated from a high speed steady flight by pitching-up the helicopter for a rapid gain in altitude. Unlike the pop-up maneuver, in which collective is initiated to accelerate vertically, longitudinal shaft tilt is initiated to pitch-up the helicopter that

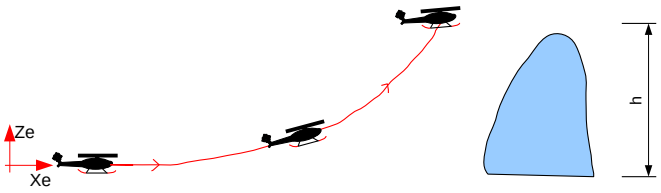

Fig. 6. Picture depicting pull-up maneuver

results in an upward tilt in rotor thrust vector causes vertical acceleration. Pull-up maneuver is depicted in Fig. 6

The maneuver being simulated is the counter 11029 flight from UH-60A flight test database. During this maneuver a maximum load factor of 2.12g was attained. The maneuver lasted for 9 seconds covering 40 rotor revolutions. The flight test data is taken from (Refs. 21, 22). The measured load factor and velocity ratio are shown in Figs. 7 and 8. One of the key requirements of this maneuver was to maintain a load factor of 1.75g for 3 seconds with less than 15 m/s loss in airspeed. The helicopter attitude angles and angular rates are shown in Figs. 9 and 10 respectively, with negative representing the nose down attitude.

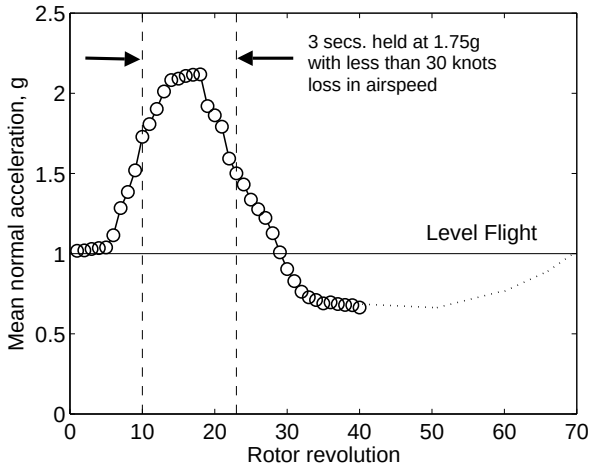

Fig. 7. Picture depicting Measured mean load factor for pull-up maneuver

Like any other constant forward velocity maneuver, trajectory of pull-up maneuver also can be defined by a polynomial equation. The available information is used to derive the equation for pull-up maneuver under simulation:

$$Z_e(t) = -0.047\,(t)^4 + 0.507\,(t)^3 + 7.21\,(t)^2 - 2.429t + 1.9725 \tag{20}$$

$$\dot{X}_e(t) = \sqrt{V_f^2 - \dot{Z}_e(t)^2} \tag{21}$$

The variation of longitudinal and vertical non-dimensional acceleration of helicopter, for pull-up maneuver, is shown as a function of time in Fig. 11

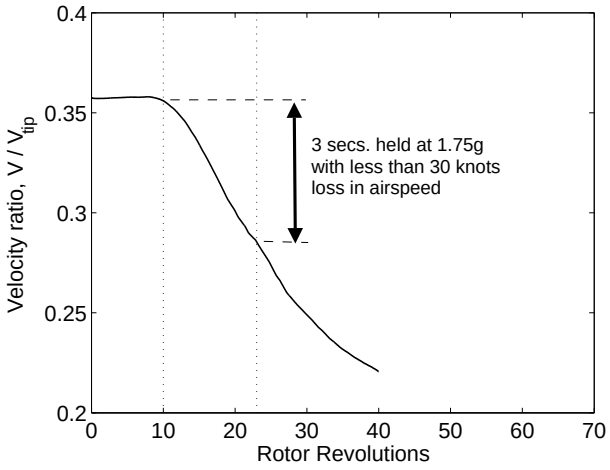

Fig. 8. Picture depicting velocity ratio for pull-up maneuver

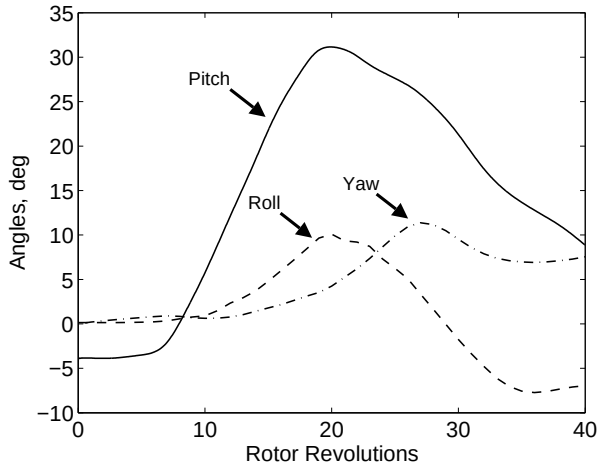

Fig. 9. Picture depicting helicopter attitude for pull-up maneuver

Bob-up Maneuver

As shown in Fig. 12 helicopter starts from hover and accelerates vertically till half of the maneuver time then decelerates to hover again by the end of the maneuver, when helicopter reaches its desired altitude. Thus helicopter reaches maximum velocity during the middle of the maneuver. The velocity of helicopter as a function of time, over this maneuver, is described by the polynomial equation (Ref. 20):

$$V(t) = V_{max}\left[-64\left(\frac{t}{t_m}\right)^6 + 192\left(\frac{t}{t_m}\right)^5 - 192\left(\frac{t}{t_m}\right)^4 + 64\left(\frac{t}{t_m}\right)^3\right] \tag{22}$$

$$\dot{X}_e(t) = 0 \tag{23}$$

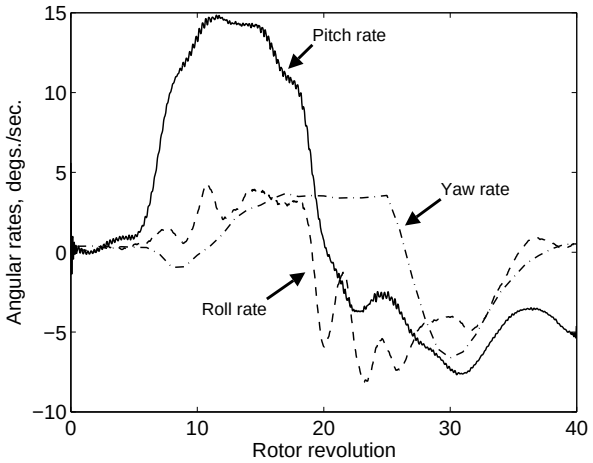

Fig. 10. Picture depicting helicopter attitude for pull-up maneuver

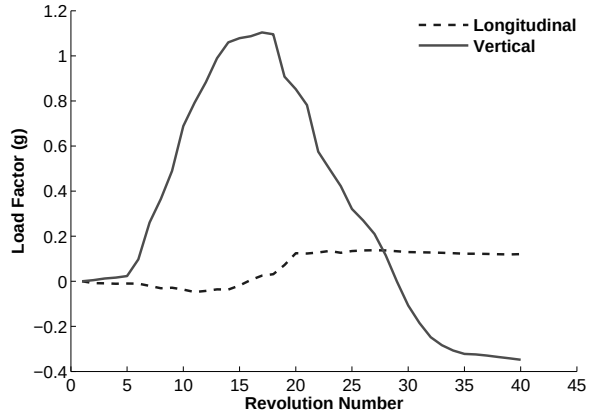

Fig. 11. Load factor variation for pull-up maneuver

Helicopter velocity profile for this maneuver is shown in Fig. 13

Pirouette Maneuver

The pirouette maneuver starts from a hover condition on a reference circumference of a pre-defined radius; the rotorcraft must then perform a lateral translation around the circumference, pointing its nose to the centre of the circle. This maneuver is depicted in Fig. 14

This maneuver is described as

$$X_e(t) = -r\cos(\omega t) \quad (24)$$
$$Y_e(t) = r\sin(\omega t) \quad (25)$$
$$Z_e(t) = 0 \quad (26)$$
$$\psi(t) = -\omega t \quad (27)$$

For the present simulation, a circle of radius(r) of 4 m with aircraft angular Velcoity(ω) of 0.5 rad/s, is chosen to carry

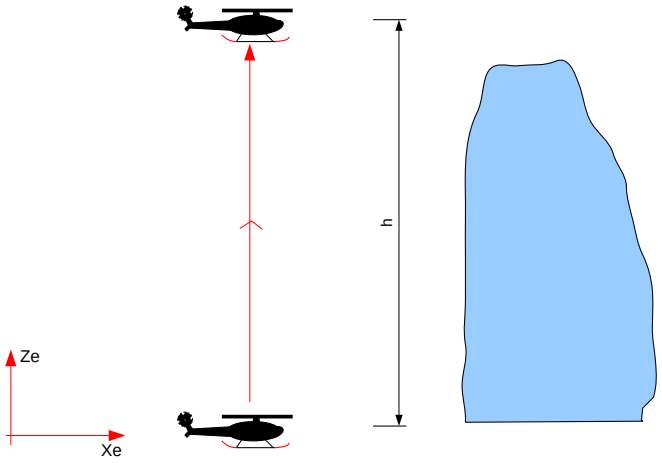

Fig. 12. Picture depicting bob-up maneuver

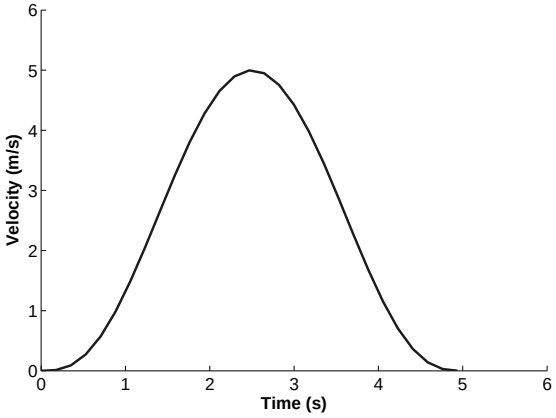

Fig. 13. Velocity profile for bob-up maneuver

out this maneuver. The required acceleration profile to be achieved by helicopter is depicted in Fig. 15

The effective parameters of various maneuvers under simulation are as given in Table 2

Table 2. Helicopter parameters used for inverse simulation

Maneuver	V_f (m/s)	t_m (s)	h (m)
Pull-up	77.76	9	152.4
Pop-up	41.16	8	25
Hurdle-hop	41.16	17.5	50
Bob-up	NA	5	NA
Pirouette	NA	12.5	NA

RESULTS

First, the inverse flight dynamics simulation is carried out for the pull-up maneuver for UH-60A helicopter as the flight test data is available in the public domain. This allows for the validation of overall methodology. Also, the analysis is carried out using linear as well as non-linear aerodynamics and the effect of non-linear aerodynamic modelling is understood.

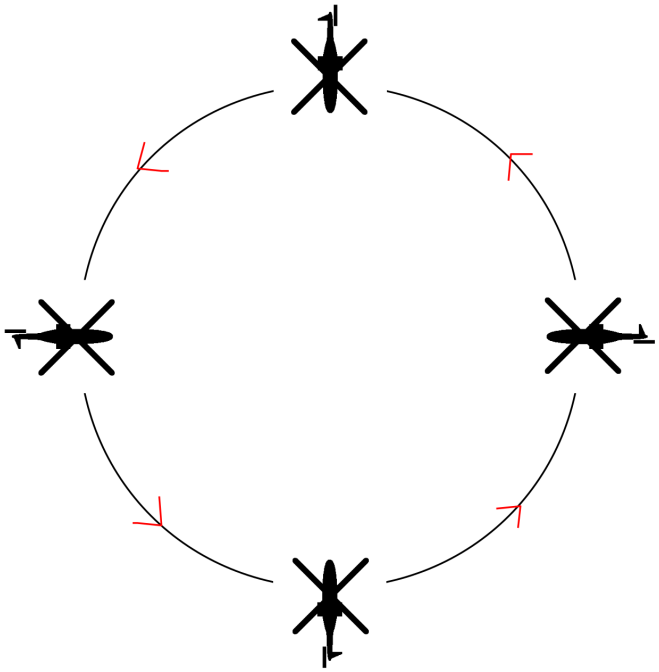

Fig. 14. Picture depicting pirouette maneuver

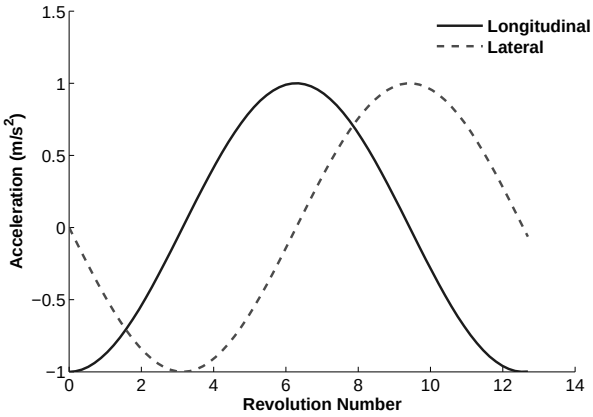

Fig. 15. Acceleration profile for pirouette maneuver

Pull-up Maneuver

The time history of measured and predicted collective, lateral cyclic and longitudinal cyclic angles are shown in Figs. 16(a), 16(b) and 16(c) respectively. The flight test collective angle shown in Fig. 16(a) is observed to remain constant during initial steady flight regime (1–5 revolutions) of the maneuver. The predicted results show similar trend during this portion of the maneuver. During the rotor revolution number 10–19, which represents a high velocity and high load factor regime of the maneuver, a significant reduction in required collective is observed despite of the increase in helicopter load factor. This is probably due to the additional inflow at the rotor due to high upward velocity of the helicopter and the analysis is able to predict this trend quite accurately. During revolutions 20–35 a gradual increase in collective control is observed despite reduction in load factor owing to the fact that additional inflow that was available to the rotor is reduced due to decrease in vertical flight velocity. Since helicopter tried to recover to its normal steady flight during last few revolutions (i.e., 32 to 40) of the maneuver, the required collective increases at a gradual rate. The inverse simulation is unable to predict this gradual increase in collective angle beyond revolution 28, instead the collective angle starts to decrease again. This may be due to the use of simple inflow model which may not be able to accurately account for the change in inflow experienced by the rotor during attitude recovery phase of the maneuver. The predicted lateral cyclic angles shown in Fig. 16(b) have similar trend as flight test, the prediction with linear aerodynamics shows best correlation in terms of peak-to-peak magnitude and trend of variation during the maneuver. The predicted control angles using airfoil look-up table based non-linear aerodynamics show a decrease in lateral cyclic angle near revolution 9–15, and shows higher peak-to-peak variation than flight test. The time history of predicted longitudinal cyclic angles using the two aerodynamics models is compared in Fig. 16(c). Both analyses capture the trend observed in the flight test data satisfactorily, but the predictions show significant mean offset when compared to flight test. The magnitude of the longitudinal cyclic mean estimated using linear aerodynamics is overpredicted by 2.9° and that using non-linear aerodynamics is overpredicted by 3.7° approximately. The predictions with corrected mean values are also shown in the Fig. 16(c) for comparing the peak-to-peak magnitude variation. The prediction for longitudinal cyclic obtained using non-linear aerodynamics has peak-to-peak variation similar to that observed for flight test. In general, the predicted control angles obtained using non-linear static stall based aerodynamics shows larger variation in peak-to-peak magnitude. This may be due to decrease in lift with increase in angle of attack with onset of static stall at various blade sections which may require the whole blade to be operated at overall higher pitch angles.

Figure 17 shows the longitudinal and lateral shaft tilt angles predicted by the inverse simulation. Both predictions show trends similar to flight test. The peak-to-peak magnitudes are significantly underpredicted. The predictions from the linear aerodynamics show better correlation than the predictions obtained using non-linear aerodynamics.

Fig. 18 compares the estimated helicopter body force targets with the actual forces achieved during the inverse simulation. Corresponding roll and pitch moment comparison is shown in Fig. 19. It is observed that the hub-forces and moments achieved by the inverse simulation are nearly identical to the estimated target loads from flight test data.

It appears that using a non-linear static stall based aerodynamic model for an unsteady pull-up maneuver characterized by deep stall condition is not a good choice, and therefore, linear aerodynamic model without stall is better suited for unsteady maneuver analysis when compared to static airfoil table lookup. Incorporation of unsteady aerodynamics may be a more appropriate refinement. For all subsequent analysis for

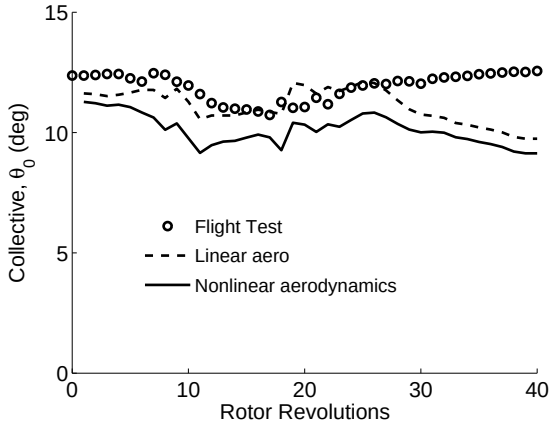

(a) Collective, θ_0

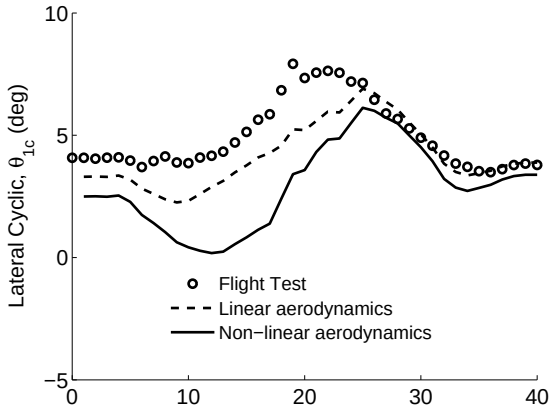

(b) Lateral Cyclic, θ_{1c}

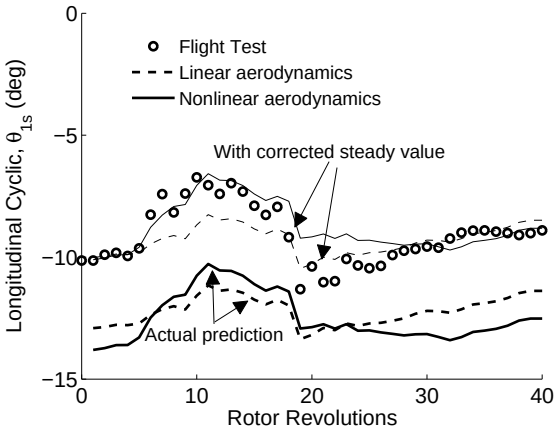

(c) Longitudinal Cyclic, θ_{1s}

Fig. 16. Measured and predicted control angles using inverse simulation for pull-up maneuver for UH-60A helicopter

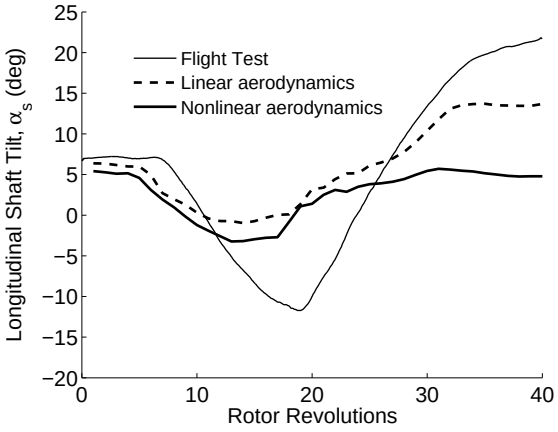

(a) Longitudinal shaft tilt, α_s

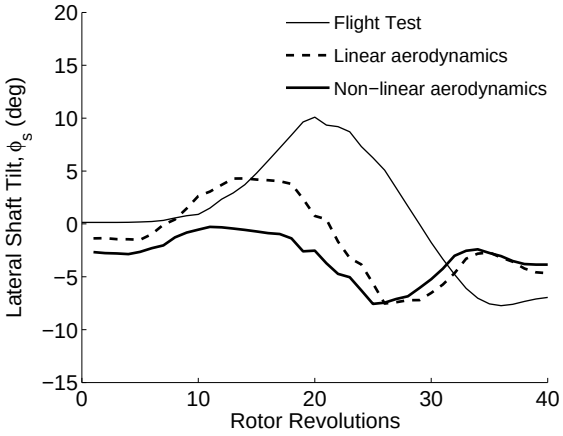

(b) Lateral shaft tilt, α_c

Fig. 17. Measured and predicted shaft tilt angles using inverse simulation for pull-up maneuver

Lynx helicopter, linear aerodynamics model is used.

Since the derived sequence of controls are matching satisfactorily with the flight test results, other maneuvers, those mentioned in previous section, are simulated for Westland Lynx helicopter.

Pop-up Maneuver

Pop-up maneuver is initiated by increasing the collective to lift-up the helicopter in the initial phase of the maneuver in which helicopter is accelerated vertically as shown in Fig. 20. It is also observed that, the lateral forces are of low magnitude and hence the variation of lateral cyclic, θ_{1c} is small. The increased collective makes the helicopter climb rapidly which would result in forward acceleration. The tendency of the tip path plane is to tilt backwards due to increase in lift on the advancing side and decrease in lift on the retreating side. This is compensated by increasing the magnitude of negative longitudinal cyclic as shown in Fig. 20. The present analysis is able to capture this trend and shows fair correlation with the predicted results from (Ref. 23).

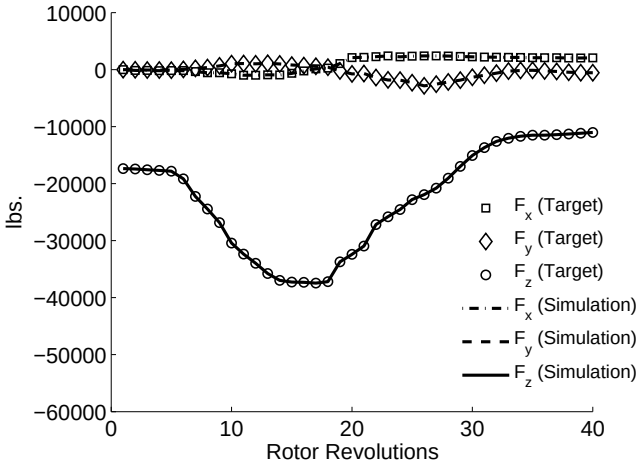

Fig. 18. Calculated and achieved helicopter hub forces in body fixed frame using measured flight test data

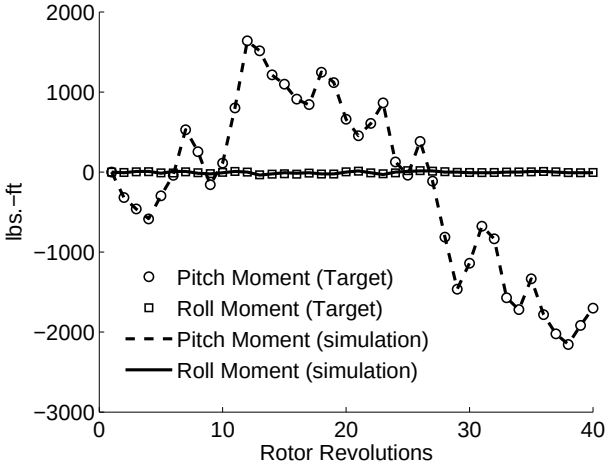

Fig. 19. Calculated and achieved helicopter hub moments in body fixed frame using measured flight test data

The simulated vehicle attitudes (roll and pitch) for this maneuver are shown in Fig. 21. As mentioned earlier pop-up maneuver is primarily a 2D maneuver where there is very little lateral motion as shown by nearly constant lateral attitude during this maneuver. The control variation discussed above result in nose-up pitching motion in the initial phase (up to 12 revolutions) of flight. A gradual reduction in vertical acceleration combined with reduction in forward deceleration makes the helicopter return to its initial pitch attitude by half time point of maneuver when load factor on helicopter reaches back to its initial steady state value. The helicopter pitch orientation during the second half of the maneuver is opposite to that of the first half as the acceleration varies in opposite manner. Helicopter returns to its initial orientation of steady state by the end of the maneuver.

As there is no lateral motion in the simulated pop-up maneuver, tail rotor has to just counteract the main rotor torque

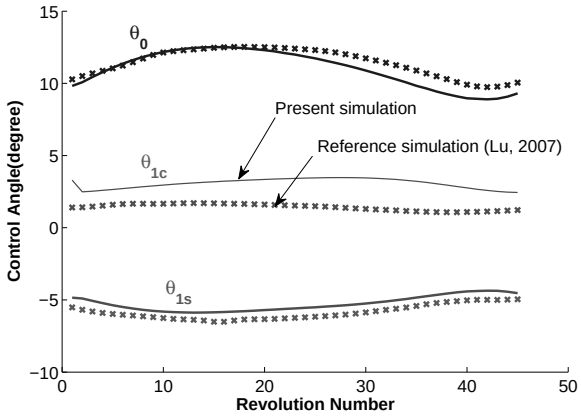

Fig. 20. Simulated and reference (Lu.,L, (Ref. 23)) controls for pop-up maneuver

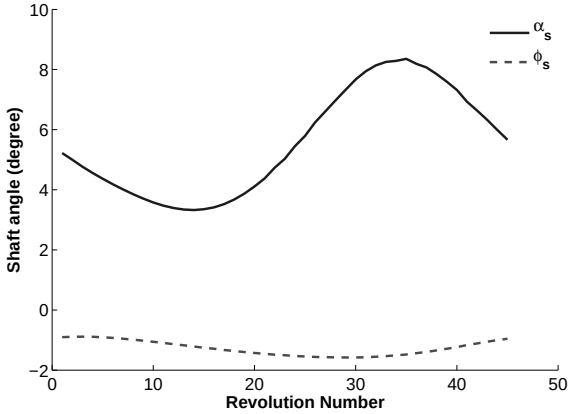

Fig. 21. Simulated shaft angles for pop-up maneuver

which is mainly a function of main rotor collective. Therefore, the variation of tail rotor collective shown in Fig. 22 follows the trend of the required main rotor collective. The variation of simulated tail rotor collective is similar to that obtained by (Ref. 23). The peak-to-peak magnitude is underpredicted by 1°. This may be because of the differences in the tail rotor modelling between the two analyses. The exact details of tail rotor model used in (Ref. 23) is not available.

Hurdle-hop Maneuver

In hurdle-hop maneuver helicopter tries to regain its initial altitude following a gain in altitude during the first half of the maneuver. Figure 23 shows the predicted time history of control angles required to simulate this maneuver. It is observed that the maneuver requires a gradual increase in vertical acceleration during first quarter (up to 24 rotor revolutions) of maneuver requiring an increase in collective pitch which is then followed by a deceleration until it reaches the apex of the trajectory at the desired altitude. Hence collective is reduced during the second quarter. The third quarter witnesses further reduction in collective followed by an increase, which

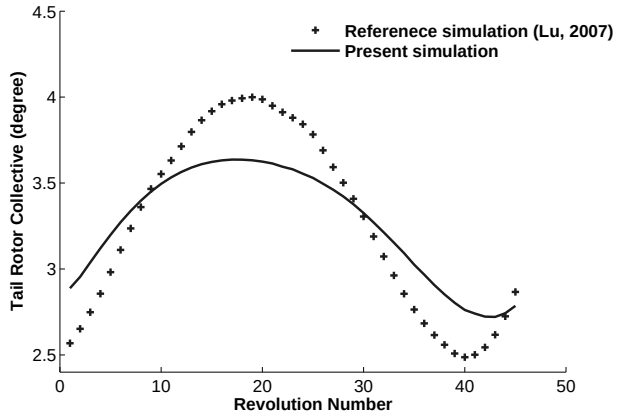

Fig. 22. Simulated tail rotor collective for pop-up maneuver

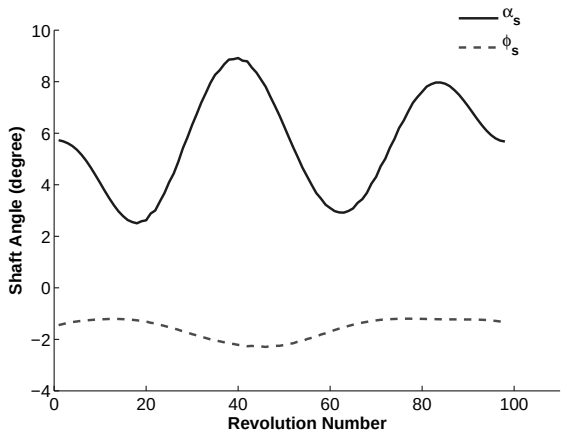

Fig. 24. Simulated shaft angles for hurdle-hop maneuver

continues till the end of the maneuver as the helicopter tries to attain the original trim state. The longitudinal cyclic has to be adjusted which requires initial decrease and then increase followed by further reduction to allow the helicopter to first decelerate during the climb process and then after the correct altitude is attained it accelerates on its way back to original altitude. The trends for collective and longitudinal cyclic angles are similar to that predicted by (Ref. 23). The lateral cyclic angle shows greater peak-to-peak variation than the reference predictions. The reason for this is not fully understood.

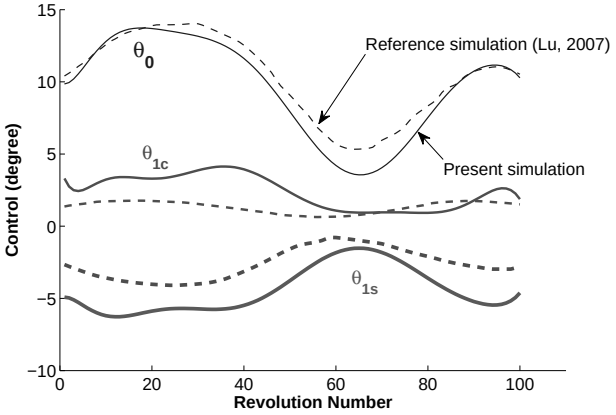

Fig. 23. Simulated and reference (Lu.,L, (Ref. 23)) controls for hurdle-hop maneuver

The simulated vehicle attitudes for this maneuver are shown in Fig. 24. Helicopter is initially pitching-up to be consistent with the changing moments due to increasing vertical acceleration and corresponding forward deceleration which is then followed by a gradual reduction in pitch angle to meet the required forward acceleration and corresponding vertical deceleration leading to initial helicopter orientation by the time helicopter reaches the apex of the maneuver where longitudinal velocity would be maximum again with zero climb velocity.

Hurdle-hop maneuver is also primarily a longitudinal maneuver, therefore the tail rotor collective follows the main rotor torque requirement which in turn follows the main rotor collective as shown in Fig. 25.

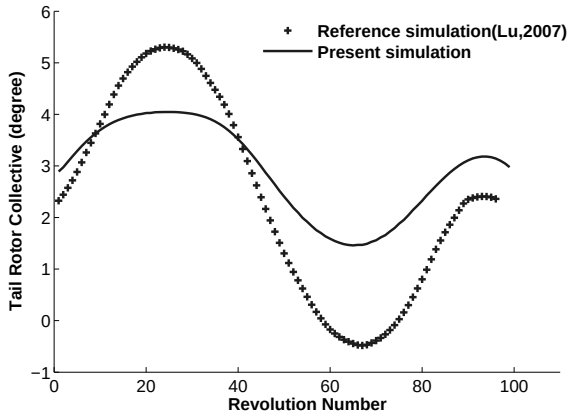

Fig. 25. Simulated shaft angles for hurdle-hop maneuver

Bob-up Maneuver

The bob-up maneuver is practically a 1D maneuver involving axial flight, in which the helicopter is in hover condition from which it is moved to hover condition at higher altitude. This requires the helicopter to accelerate vertically upwards and then decelerate to return to hover. This is achieved by changing the collective in near sinusoidal manner as shown in Fig. 26. Thus the aircraft acceleration is zero around the middle of the maneuver after which helicopter starts decelerating requiring a decrease in collective. Variation in cyclic controls is negligible due to the absence of any longitudinal or lateral motion during the maneuver.

The variation of longitudinal and lateral shaft tilt angles for Bob-up maneuver is shown in Fig. 27. As expected the at-

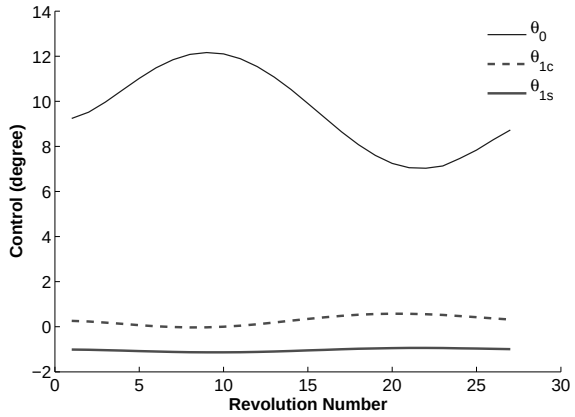

Fig. 26. Simulated controls for bob-up maneuver

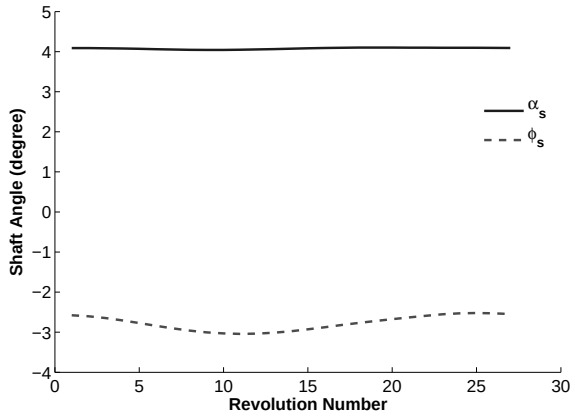

Fig. 27. Simulated shaft angles for bob-up Maneuver

titude of the helicopter remains unchanged during the maneuver. The variation of tail rotor collective is shown in Fig. 28. During the initial phase of maneuver collective is gradually increased to balance the increasing main rotor torque. After the initial acceleration phase tail rotor collective also decreases along with decreasing power requirement from main rotor.

Pirouette Maneuver

Since the maneuver is of very low speed with a resultant velocity of 2 m/s in horizontal plane with a rotational speed of 0.5 rad/s, the collective is nearly constant through out the maneuver. The periodic velocity in longitudinal and lateral directions result in periodically varying cycling controls as shown in Fig. 29.

The simulated shaft angles for pirouette maneuver shown in Fig. 30 variation of longitudinal shaft tilt reflects the variation of longitudinal acceleration required by maneuver. Since collective remains nearly constant, tip path plane has to be tilted forward and side-wards to accelerate the vehicle during first half of the maneuver and reversed back to its initial orientation by end of the maneuver. Similarly lateral shaft tilt varies periodically to achieve periodically varying lateral

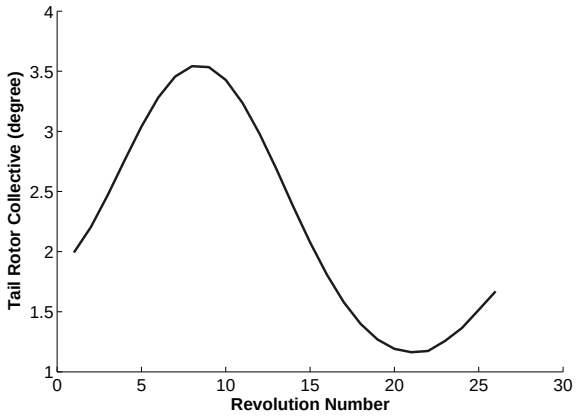

Fig. 28. Simulated tail rotor collective for bob-up maneuver

force to enable the flight in a circular path. The variation of tail rotor collective is shown in Fig. 31. The tail rotor collective plays a crucial role in maintaining a constant yaw rate during this maneuver.

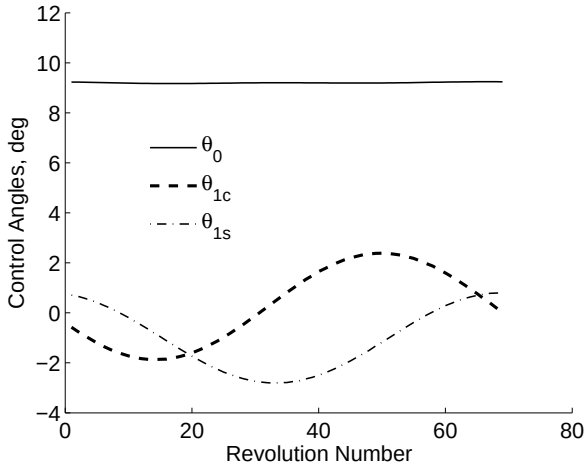

Fig. 29. Simulated controls for pirouette maneuver

SUMMARY & CONCLUSIONS

The implementation of integration based inverse simulation algorithm is discussed in this paper. The analysis is validated by simulating UH-60A Black Hawk helicopter for 2.1g dynamic pull-up maneuver. The results for various maneuvers, including pop-up and hurdle-hop maneuvers, are simulated for controls time history for Westland Lynx helicopters and compared with simulation results available in literature. Finally, bob-up and pirouette maneuver is also analyzed. The conclusions drawn from this analysis are listed below:

1. A simple helicopter dynamics model consisting of articulated blades with linear twist, quasi-steady linear aerodynamics with Drees inflow model is adequate to study

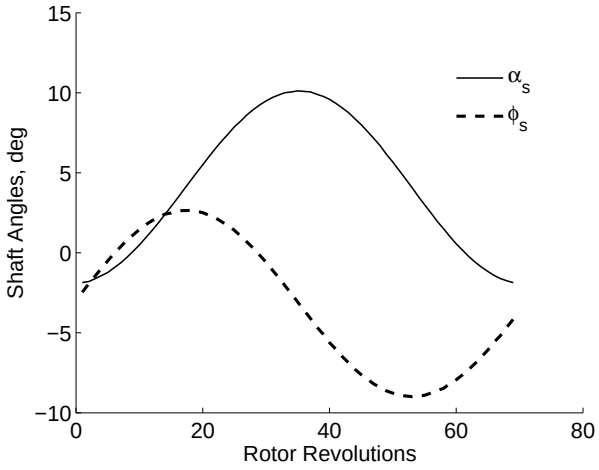

Fig. 30. Simulated shaft angles for pirouette maneuver

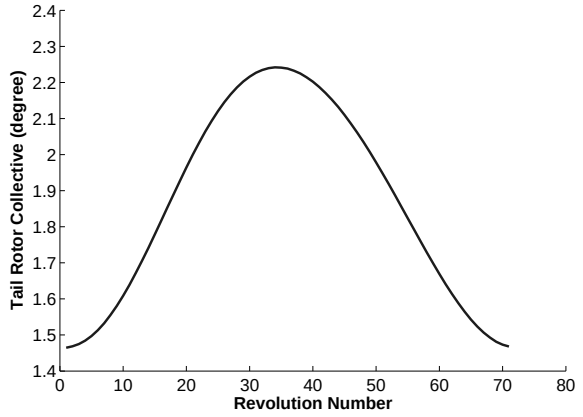

Fig. 31. Simulated tail rotor collective for pirouette maneuver

the behaviour of helicopter performing unsteady maneuvers.

2. The generalized intergation based inverse simulation is successfully validated and verified for unsteady maneuvers performed by two different helicopters and five different maneuver. The predicted controls show fair correlation with flight test controls (in the case of pull-up maneuver) and reference controls in magnitude and variation. However, magnitudes of tail rotor collective are underpredicted, possibly due to differences in tail rotor modelling.

3. For all symmetric maneuvers such as pull-up, pop-up, bob-up, and hurdle-hop maneuvers the tail rotor collective follows the trend of collective pitch control.

4. It is observed that the variation of pitch orientation follows the trend of the vertical acceleration of the helicopter.

REFERENCES

[1]Kato, O., and Sugiura, I.,"An Interpretation of Airplane General Motion and Control as Inverse Problem,"*Journal of Guidance*, Vol. 9, No. 2, 1985, pp.198–204.

[2]Lane, S.H., and Stengel, R.,"Flight Control Design Using Non-linear Inverse Dynamics,"*Automatica*, Vol. 24, No. 4, 1988, pp.471-483.

[3]Thomson, D.G., and Bradley, R., "Recent Developments in the Calculation of Inverse Solutions of the Helicopter Equations of Motion," Proceedings of the UK simulation Council Triennial Conference, September 1987.

[4]Thomson, D.G., and Bradley, R., "Development and Verification of an Algorithm for Helicopter Inverse Simulation," *Vertica*, Vol. 14, No. 2, 1990, pp. 185–200.

[5]Hess, R.A., Gao, C., and Wang, H.S., "Generalized Technique for Inverse Simulation Applied to Aircraft Maneuvers," *Journal of Guidance, Control, and Dynamics*, Vol. 14, No. 5, SeptemberOctober 1991, pp. 920–926.

[6]Hess, R.A., Gao, C., "A Generalized Algorithm for Inverse Simulation Applied to Helicopter Maneuvering Flight," *Journal of the American Helicopter Society*, Vol. 38, No. 3, October 1993, pp. 3–15.

[7]K. C. Lin, and P. Lu.,"Inverse Simulation - An Error Analysis," *SIMULATION*, Vol. 65, No. 6, Dec 1995, pp. 385-392.

[8]Matteis, G., Socio, L., and Alexander, L.,"Solution of Aircraft Inverse problems by Local Optimization," *Journal of Guidance, Control and Dynamics*, Vol. 18, No. 3, May-June 1995.

[9]Avanzini, G., and de Matteies, G.,"Two-Timescale Inverse Simulation of a Helicopter Model," *Journal of Guidance, Control and Dynamics*, Vol. 24, No. 2, March–April 2001, pp. 330–339.

[10]Celi, R., "Optimization-Based Inverse Simulation of a Helicopter Slalom Maneuver", *Journal of Guidance, Control and Dynamics*, Vol. 23, No.2, March-April 2000.

[11]Lee, S., and Kim, Y., "Time-Domain Finite Element Method for Inverse Problem of Aircraft Maneuvers," *Journal of Guidance, Control and Dynamics*, Vol. 20, No.1, January-February 1997.

[12]Lu, L., and Murray, D.J.-Smith.,"Sensitivity-Analysis Method Inverse Simulation Application," *Journal of Guidance, Control and Dynamics*, Vol. 30, No.1, January-February 2007.

[13]Guglieri, G., and Mariano, V., "Optimal Inverse Simulation of Helicopter Maneuvers," *Communications to SIMAI Congress*, Vol. 3, 2009, pp. 261–272.

[14]Dai, J., Wu, G., Wu, Y., and Zhu, G., "Helicopter Trim Research Based on Hybrid Genetic Algorithm," 7th World Congress on Intelligent Control and Automation, pp. 2007–2011, 25–27 June 2008.

[15]Davis, S. J., "Predesign Study for a Modern 4-Bladed Rotor for the RSRA," NASA CR-166155, March 1981.

[16]Bousman, W. G., "Aerodynamic Characteristics of SC1095 and SC1094 R8 Airfoils," NASA TP-2003-212265, December 2003.

[17]Howlett, J. J., "UH-60A Black Hawk Engineering Simulation Program," NASA CR 166309, December 1981.

[18]Kufeld, R. M., Balough, D. L., Cross, J. L., Studebaker, K. F., Jennison, C. D., and Bousman, W. G., "Flight Testing of the UH-60A Airloads Aircraft," American Helicopter Society 50th Annual Forum Proceedings, Washington, D. C., May 1994.

[19]Yeo, H., Bousman, W. G., and Johnson, W., "Performance Analysis of a Utility Helicopter with Standard and Advanced Rotors," *Journal of American Helicopter Society*, Vol. 49, No. 3, July 2004, pp. 250–270.

[20]Thomson, D.G., and Bradley, R., "Mathematical Definition of Helicopter Maneuvers,"*Journal of The Americal Helicopter Society*, Vol. 42, No.4, October 1997, pp.307–309.

[21]Bhagwat, M. J., Ormiston, R. A., Saberi, H. A., and Xin, H., "Application of Computational Fluid Dynamics/Computational Structural Dynamics Coupling for Analysis of Rotorcraft Airloads and Blade Loads in Maneuvering Flight," *Journal of the American Helicopter Society*, Vol. 57, No. 3, July 2012, pp. 1–21.

[22]Abhishek, Datta, A., Ananthan, S., and Chopra, I., "Prediction and Analysis of Main Rotor Blade Loads in a Prescribed Pull-Up Maneuver," *Journal of Aircraft*, Vol. 47, No. 4, July–August 2010, pp. 1197–1215.

[23]Lu, L., " Inverse Modelling and Invere Simulation for System Engineering and Control Applications," *Ph.D. Dissertation*, Department of Electronics and Electrical Engineering, University of Glasgow, October 2007.